Draft version February 1, 2008
Preprint typeset using LaTeX style emulateapj v. 10/09/06

THE JOINT LARGE-SCALE FOREGROUND—CMB POSTERIORS OF THE 3-YEAR WMAP DATA

H. K. Eriksen[1,2,3], C. Dickinson[4], J. B. Jewell[4], A. J. Banday[5], K. M. Górski[4,7], C. R. Lawrence[4]

(Dated: Received - / Accepted -)
Draft version February 1, 2008

ABSTRACT

Using a Gibbs sampling algorithm for joint CMB estimation and component separation, we compute the large-scale CMB and foreground posteriors of the 3-yr WMAP temperature data. Our parametric data model includes the cosmological CMB signal and instrumental noise, a single power law foreground component with free amplitude and spectral index for each pixel, a thermal dust template with a single free overall amplitude, and free monopoles and dipoles at each frequency. This simple model yields a surprisingly good fit to the data over the full frequency range from 23 to 94 GHz. We obtain a new estimate of the CMB sky signal and power spectrum, and a new foreground model, including a measurement of the effective spectral index over the high-latitude sky. A particularly significant result is the detection of a common spurious offset in all frequency bands of $\sim -13\,\mu$K, as well as a dipole in the V-band data. Correcting for these is essential when determining the effective spectral index of the foregrounds. We find that our new foreground model is in good agreement with template-based model presented by the WMAP team, but not with their MEM reconstruction. We believe the latter may be at least partially compromised by the residual offsets and dipoles in the data. Fortunately, the CMB power spectrum is not significantly affected by these issues, as our new spectrum is in excellent agreement with that published by the WMAP team. The corresponding cosmological parameters are also virtually unchanged.

Subject headings: cosmic microwave background — cosmology: observations — methods: numerical

1. INTRODUCTION

A major challenge in CMB research is component separation, which can be summarized in two questions. First, how can we separate reliably the valuable cosmological signal from confusing foreground emission? Second, how can we propagate accurately the errors induced by this process through to the final analysis products, such as the CMB power spectrum and cosmological parameters?

During the last few years, a new analysis framework capable of addressing these issues in a statistically consistent approach has been developed. This framework is Bayesian in nature, and depends critically on the Gibbs sampling algorithm as its main computational engine. The pioneering ideas were described by Jewell et al. (2004) and Wandelt et al. (2004), and later implemented for modern CMB data sets for temperature and polarization by Eriksen et al. (2004a) and Larson et al. (2007), respectively. Applications to the 1-yr and 3-yr WMAP data (Bennett et al. 2003a; Hinshaw et al. 2007; Page et al. 2007) were described by O'Dwyer et al. (2004), and Eriksen et al. (2006, 2007a). These papers mainly focused on the cosmological CMB signal, and adopted the foreground corrected data provided by the WMAP team.

Recently this algorithm was extended to include internal component separation capabilities by Eriksen et al. (2007b). Using very general parameterizations of the foreground components, this method produces the full joint and exact foreground-CMB posterior, and therefore allows us both to estimate each component separately through marginalized statistics and to propagate the foreground uncertainties through to the final CMB products. The implementation of this algorithm used in this paper is called "Commander", and is a direct descendant of the code presented by Eriksen et al. (2004a).

In this Letter, we apply the method to the 3-yr WMAP temperature observations (Hinshaw et al. 2007). This data set, with five frequency bands, allows only very limited foreground models; however, the analysis provides a powerful demonstration of the capabilities of the method. For a comprehensive analysis of a controlled simulation with identical properties to this data set, see Eriksen et al. (2007b).

2. DATA

We consider the 3-yr WMAP temperature data, provided on Lambda[7] in the form of sky maps from ten "differencing assemblies" covering the frequency range between 23 and 94 GHz. Since our current implementation of the Gibbs foreground sampler can only handle sky maps with identical beam response (Eriksen et al. 2007b), we downgrade each of these maps to a common resolution of 3° FWHM and repixelize at a HEALPix[8] resolution of $N_{\rm side} = 64$, corresponding to a pixel size of $55'$. These ten maps are then co-added by frequency into five single frequency band maps at 23, 33, 41, 64 and 94 GHz (K, Ka, Q, V and W-bands, respectively).

The power from the instrumental noise is less than 1%

[1] email: h.k.k.eriksen@astro.uio.no
[2] Institute of Theoretical Astrophysics, University of Oslo, P.O. Box 1029 Blindern, N-0315 Oslo, Norway
[3] Centre of Mathematics for Applications, University of Oslo, P.O. Box 1053 Blindern, N-0316 Oslo
[4] Jet Propulsion Laboratory, California Institute of Technology, Pasadena CA 91109
[5] Max-Planck-Institut für Astrophysik, Karl-Schwarzschild-Str. 1, Postfach 1317, D-85741 Garching bei München, Germany
[6] Warsaw University Observatory, Aleje Ujazdowskie 4, 00-478 Warszawa, Poland

[7] http://lambda.gsfc.nasa.gov
[8] http://healpix.jpl.nasa.gov

of the CMB signal at $\ell = 50$ in the V- and W-bands, and less than 2% at $\ell = 100$ (Eriksen et al. 2007b). To regularize the noise covariance matrix at high spatial frequencies, we added $2\,\mu$K per 3° pixel of uniform white noise. This noise is insignificant at low multipoles, but dominates the signal near the spherical harmonic truncation limit of $\ell_{\rm max} = 150$. We then have five frequency maps at a common resolution of 3° FWHM, with signal-to-noise ratio of unity at $\ell \sim 120$, and strongly bandwidth limited at $\ell_{\rm max} = 150$.

We choose to include such high l's in the analysis for two reasons. First, our main goal is an accurate approximation of the CMB likelihood at $\ell \leq 50$. In order to ensure that the degradation process (i.e., smoothing and noise addition) does not significantly affect these multipoles, it is necessary to go well beyond $\ell \sim 80$–100. Second, significant information on the spatial distribution of foregrounds is obtained by going to higher resolution.

The cost of this treatment of the noise is high χ^2 values in the ecliptic plane (Eriksen et al. 2007b), where the instrumental noise is higher because of WMAP's scanning strategy. However, since these high χ^2 values are caused by unmodelled smoothed, random, white noise, they do not indicate a short-coming of the signal model, but only a slight under-estimation of the statistical errors on small angular scales. This has been confirmed by otherwise identical analyses at both 4° and 6° FWHM. We present the 3° FHWM case here as a compromise between angular resolution and accuracy of the noise model. This issue will further suppressed with additional years of WMAP observations and, eventually, high-sensitivity Planck maps.

We impose the base WMAP Kp2 sky cut (Bennett et al. 2003b) on the data, but not the point source cuts. The base mask is downgraded from its native $N_{\rm side} = 512$ resolution to $N_{\rm side} = 64$ by excluding all low-resolution pixels for which any one of its sub-pixels is excluded by the high-resolution mask. A total of 42 081 pixels are included, or 85.6% of the sky.

The frequency bandpass of each map is modelled as a top-hat function, and implemented in terms of effective frequency as a function of spectral index as described by Eriksen et al. (2006). The frequency specifications of the WMAP radiometers are given by Jarosik et al. (2003).

3. MODEL AND METHODS

We adopt the following simple parametric model $T_\nu(p)$ for the observed signal (measured in thermodynamic temperatures) at frequency ν and pixel p,

$$T_\nu(p) = s(p) + m_\nu^0 + \sum_{i=1}^{3} m_\nu^i \left[\hat{\mathbf{e}}_i \cdot \hat{\mathbf{n}}(p)\right] + \\ + b\left[t(p)a(\nu)\left(\frac{\nu}{\nu_0^{\rm dust}}\right)^{1.7}\right] + f(p)a(\nu)\left(\frac{\nu}{\nu_0}\right)^{\beta(p)}. \quad (1)$$

The first term is the cosmic CMB signal, characterized by a frequency-independent spectrum and a covariance matrix in spherical harmonic space given by the power spectrum, $\langle a_{\ell m}^* a_{\ell' m'}\rangle = C_\ell \delta_{\ell\ell'}\delta_{mm'}$, where $s(p) = \sum_{\ell,m} a_\ell Y_{\ell m}(p)$. The second and third terms denote a free monopole and three dipole amplitudes at each frequency. We use the standard Cartesian basis vectors projected on the sky, $\{\mathbf{1}, \mathbf{x}, \mathbf{y}, \mathbf{z}\}$, as basis functions for these four modes. The fourth term represents a template-based dust model scaled by a spectral index of $\beta = 1.7$, in which $t(p)$ is the dust template (FDS) of Finkbeiner et al. (1999), evaluated at $\nu_0^{\rm dust} = 94\,$GHz, and $a(t)$ is the conversion factor between antenna and thermodynamic temperatures. The last term is a single foreground component with a free amplitude $f(p)$ and spectral index $\beta(p)$ at each pixel. The reference frequency for this component is $\nu_0 = 23\,$GHz.

The free parameters in this model are: 1) spherical harmonic coefficients $a_{\ell m}$ of the CMB amplitude s; 2) CMB power spectrum coefficients C_ℓ; 3) monopole and dipole amplitudes at each band; 4) the amplitude of the dust template; and 5) amplitudes and spectral indices of the pixel foreground component.

The WMAP data do not have sufficient power to constrain this simple completely by themselves, as there is a very strong degeneracy between the foreground component amplitudes at each pixel and the free monopole and dipole coefficients at each band (Eriksen et al. 2007b). For this reason, we introduce two priors in addition to the Jeffereys' ignorance prior discussed by Eriksen et al. (2007b). First, we impose a Gaussian prior on the spectral indices of $\beta \sim -3 \pm 0.3$: A direct fit of the 408 MHz template (Haslam et al. 1981) to the WMAP K-band data for Kp2 sky coverage implies an index of -3 (Davies et al. 2006), and Davies et al. (1996) determined a typical range for high latitude spectral indices between 408 MHz and 1420 MHz of -2.8 to -3.2. Note that this prior has a noticeable effect only at high Galactic latitudes, where the absolute foreground amplitude is low. At low galactic latitudes, the data dominate the prior by up to a factor of ~ 50, and any potential bias in the near-plane free-free regions is negligible.

Second, we impose an implicit spectral index orthogonality prior on the monopole and dipole coefficients, as described by Eriksen et al. (2007b), projecting out the frequency component of these coefficients that matches the free spectral index map, thus effectively determining the zero-level of the foreground amplitude map. We also tried an alternative approach, first estimating the Q, V, and W-band monopole and dipole coefficients separately given a crude estimate of the spectral index map, and then estimating all other parameters given these coefficients. Results were very similar. Thus, the two priors adopted in this analysis have a very weak effect on all main results.

Having defined our model and priors, we map out the joint posterior distribution using the foreground Gibbs sampler described by Eriksen et al. (2007b). We refer the interested reader to that paper for full details of the algorithm, and for a comprehensive analysis of a realistic simulation corresponding to the same data and model used in this Letter.

Finally, we estimate a new set of cosmological parameters within the standard ΛCDM model. For this analysis, we follow the approach of Eriksen et al. (2007a), and replace the low-ℓ part of the WMAP likelihood with a new Blackwell-Rao Gibbs-based estimator (Chu et al. 2005). No ancillary data sets beyond the 3-yr WMAP temperature and polarization data are included in the analysis. The CosmoMC code (Lewis & Bridle 2002) is used as the

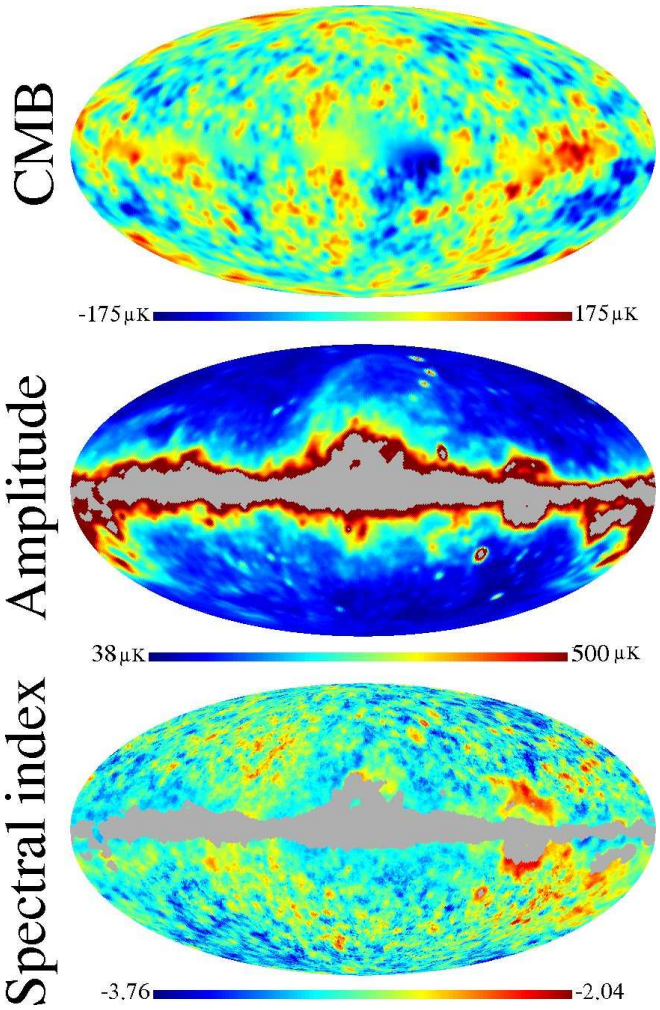

FIG. 1.— Marginal posterior mean maps in Galactic coordinates. Rows from top to bottom show the CMB reconstruction, the foreground amplitude, and the foreground spectral index, respectively.

TABLE 1
MONOPOLE AND DIPOLE POSTERIOR STATISTICS

Band	Monopole (μK)	Dipole X (μK)	Dipole Y (μK)	Dipole Z (μK)
K-band	-11.8 ± 0.5	1.7 ± 1.2	-2.2 ± 0.8	2.2 ± 0.1
Ka-band	-16.6 ± 0.5	0.9 ± 1.2	0.9 ± 0.8	-1.3 ± 0.1
Q-band	-12.8 ± 0.5	1.9 ± 1.2	-0.9 ± 0.8	0.4 ± 0.1
V-band	-11.1 ± 0.5	1.6 ± 1.2	-3.9 ± 0.8	4.0 ± 0.1
W-band	-12.6 ± 0.5	1.7 ± 1.2	-0.9 ± 0.8	1.0 ± 0.1

NOTE. — Means and standard deviations of the marginal monopole and dipole posteriors.

main MCMC engine.

4. RESULTS

Figure 1 shows the marginal posterior mean maps for the CMB sky signal, the foreground amplitude and the foreground spectral index. Table 1 gives the corresponding results for the monopole and dipole coefficients for each frequency band. The FDS dust template amplitude relative to 94 GHz and an assumed spectral index of $\beta = 1.7$ is $b = 0.917 \pm 0.003$. The CMB power spectrum is discussed separately below.

Figure 2 shows the average χ^2 computed for each Gibbs sample. A χ^2 value exceeding $\chi^2 = 15$ corresponds to

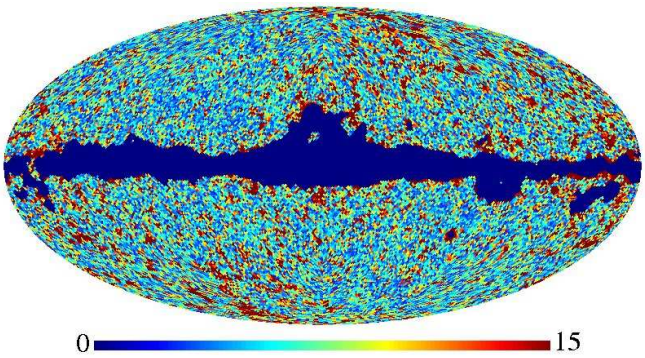

FIG. 2.— Mean χ^2 map computed over posterior samples in Galactic coordinates. A value of $\chi^2 = 15$ is high at the 99% significance level.

rejection of the model in that pixel at 99% statistical significance. Two features are clearly visible in this plot. First, the ecliptic plane, or rather, WMAP's scanning strategy, is clearly visible, and this is mainly due to the unmodelled smoothed noise component at high ℓ's, as discussed in Section 2.

Second, there are clearly visible structures near the Galactic plane, and in particular around regions with known high free-free emission (e.g., the Orion and Ophiucus regions). This is likely due to the fact that a single power-law is not a good approximation to the sum of many foregrounds with comparable amplitudes. Thus, we have clear evidence of modelling errors in this solution, and we therefore strongly emphasize that the quoted error bars presented in this paper include formal statistical errors only, and not systematic, model-dependent uncertainties. These issues are discussed in depth by Eriksen et al. (2007b), who find similar behaviour for a controlled, simulated data set.

Although χ^2 is high, the CMB solution obtained is evidently good. First of all, in the ecliptic poles, where the WMAP instrumental noise is suppressed by the scanning strategy, the χ^2 distribution is essentially perfect. This implies that the signal model as such is adequate at high latitudes. Second, the CMB map is virtually without signatures of residual foregrounds. (Note that the signal inside the Galactic plane is partially reconstructed using high-latitude information and the assumption of isotropy. The signal on scales smaller than the mask size is washed out because it is not possible to predict these from higher latitudes.) Finally, the foreground amplitude and spectral index maps correlate very well with known templates of synchrotron and free-free emission. For instance, the spectral index near the Gum nebula and near the Vela regions are close to $\beta = -2.1$, as expected for free-free emission.

The single most surprising aspects of the solution are the monopole and, possibly, the V-band dipole coefficients, listed in Table 1. Most notably, there is a strong detection of a roughly 13μK offset common to all frequency bands. Formally speaking, these offset values are only optimal within the current model; however, this type of signal is not degenerate with any other component in the model. Further, we have attempted to fit several other models assuming no offsets at one or more bands. These all result in strong, visible residuals in the CMB map, and considerably higher χ^2 values overall. Finally, very similar results have been obtained by

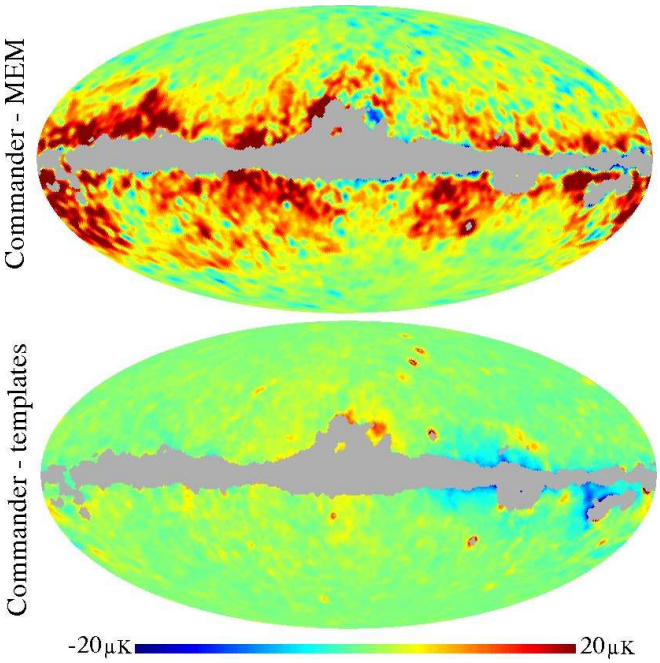

FIG. 3.— Difference maps of the total "Commander" W-band foreground model with the WMAP MEM model (top panel) and with the WMAP template fit model (bottom panel).

other researchers[9] through other methods, although, to our knowledge, these results have not yet been published in the literature. We therefore believe that the monopole and dipole coefficients presented here are more optimal even in an absolute sense than those obtained by WMAP based on a cosecant fit to a plane parallel galaxy model (Bennett et al. 2003b).

Figure 3 shows the difference maps between the Commander W-band foreground model and the MEM and template-based foreground models of Hinshaw et al. (2007). Clearly, our foreground model agrees surprisingly well with the simple template fits, but not with the MEM solution. One possible explanation for this is that although the MEM approach of Hinshaw et al. (2007) does attempt to estimate spectral indices for each pixel, it does not include monopole or dipole components in its model. Therefore, the MEM solution is plausibly compromised by the non-zero offset detected here, at least in part. In addition, the MEM method could be biased by the initial subtraction of the (foreground contaminated) ILC estimate of the CMB anisotropy from the frequency maps, and the use of the 408 MHz data as a prior. Conversely, Commander could be compromised to some extent by the use of power law spectral indices for the combined low frequency foreground component. Nevertheless, the difference is surprising given that the W-band foreground is expected to be mostly comprised of thermal dust emission.

The marginal maximum posterior CMB power spectrum is shown in Figure 4, together with the maximum-likelihood/ pseudo-C_ℓ hybrid spectrum computed by the WMAP team. Perhaps the most notable difference is in the $\ell = 21$ multipole, which looks anomalous in the WMAP spectrum, as noted by other authors.

The cosmological parameters corresponding to the

[9] See discussion lead by P. Leahy at http://cosmocoffee.info/viewtopic.php?t=631.

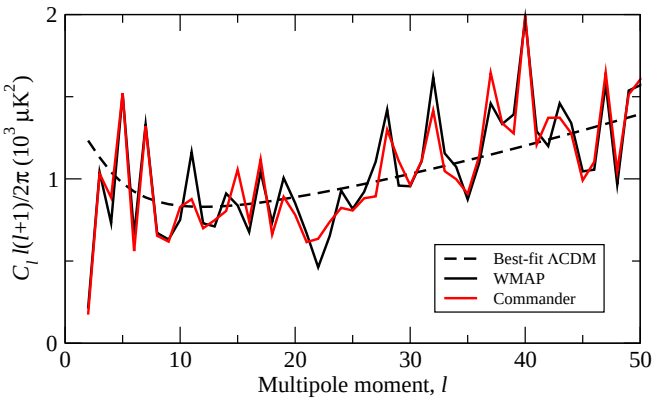

FIG. 4.— The CMB temperature power spectra obtained in this paper (red) and that by the WMAP team (black). The best-fit ΛCDM model spectrum of Spergel et al. (2007) is shown as a dashed line.

Commander spectrum for a standard six-parameter ΛCDM model are $\Omega_b\, h^2 = 0.0222 \pm 0.0007$, $\Omega_m = 0.243 \pm 0.036$, $\log(10^{10} A_s) = 3.027 \pm 0.068$, $h = 0.730 \pm 0.032$ and $\tau = 0.089 \pm 0.030$. Corresponding values for the unmodified WMAP likelihood are $\Omega_b\, h^2 = 0.0221 \pm 0.0007$, $\Omega_m = 0.242 \pm 0.035$, $\log(10^{10} A_s) = 3.030 \pm 0.068$, $h = 0.730 \pm 0.032$ and $\tau = 0.091 \pm 0.030$. These values refer to marginal means and standard deviations.

Clearly, the agreement between the two sets of results is excellent, and this provides a strong confirmation of the WMAP results: At the level of precision of the WMAP experiment, details in the foreground model used for foreground correction appear to have only a minor impact on the CMB temperature power spectrum.

5. CONCLUSIONS

We have presented the first exact Bayesian joint foreground-CMB analysis of the 3-yr WMAP data. We have established a new estimate of both the CMB sky signal and the power spectrum, a detailed foreground model consisting of a foreground amplitude and spectral index map and a dust template amplitude, and also provided new estimates of the residual monopole and dipole coefficients in the WMAP data.

The detection of significant non-zero offsets in the WMAP data is the new result of the greatest immediate importance for the CMB community. These new monopole and dipole estimates could have a significant impact on several previously published results, especially those concerning the foreground composition in the WMAP data. For example, our foreground model is in excellent agreement with the simple template fits presented by Hinshaw et al. (2007), but not with their MEM reconstruction.

Taking a longer perspective, the most important aspect of this analysis is a demonstration of feasibility of exact and joint foreground-CMB analysis. This will be essential for Planck, whose high sensitivity and angular resolution demand more accurate foreground separation than WMAP. Considering the flexibility, power, and accuracy of the method employed in this paper, together with its unique capabilities for propagating uncertainties accurately all the way from the postulated foreground model to cosmological parameters, we believe that this should be the baseline analysis strategy for Planck on large angular scales, say $\ell \lesssim 200$.

All results presented in this paper and the basic Gibbs samples are available at http://www.astro.uio.no/∼hke.

We acknowledge use of the HEALPix software (Górski et al. 2005) and analysis package for deriving the results in this paper. We acknowledge use of the Legacy Archive for Microwave Background Data Analysis (LAMBDA). This work was partially performed at the Jet Propulsion Laboratory, California Institute of Technology, under a contract with the National Aeronautics and Space Administration. HKE acknowledges financial support from the Research Council of Norway.

REFERENCES

Bennett, C. L. et al. 2003a, ApJS, 148, 1
Bennett, C. L., et al. 2003b, ApJS, 148, 97
Chu, M., Eriksen, H. K., Knox, L., Górski, K. M., Jewell, J. B., Larson, D. L., O'Dwyer, I. J., & Wandelt, B. D. 2005, Phys. Rev. D, 71, 103002
Davies, R. D., Watson, R. A. & Gutierrez, C. M. (1996), MNRAS, 278, 925
Davies, R. D., Dickinson, C., Banday, A. J., Jaffe, T. R., Górski, K. M. & Davis, R. J. 2006, MNRAS, 370, 1125
Eriksen, H. K., et al. 2004a, ApJS, 155, 227
Eriksen, H. K., Banday, A. J., Górski, K. M., & Lilje, P. B. 2004b, ApJ, 612, 633
Eriksen, H. K., et al. 2006, ApJ, 641, 665
Eriksen, H. K., Huey, G., Banday, A. J., Górski, K. M., Jewell, J. B., O'Dwyer, I. J., & Wandelt, B. D. 2007a, ApJ, 665, L1
Eriksen, H. K., Jewell, J. B., Dickinson, C., Banday, A. J., Górski, K. M., & Lawrence, C. R. 2007b, submitted, ApJ, [arXiv:0709.1058]
Finkbeiner D.P., Davis M., & Schlegel D.J. 1999, ApJ, 524, 867
Finkbeiner, D. P. 2003, ApJS, 146, 407
Górski, K. M., Hivon, E., Banday, A. J., Wandelt, B. D., Hansen, F. K., Reinecke, M., & Bartelmann, M. 2005, ApJ, 622, 759
Haslam C.G.T., Klein U., Salter C.J., Stoffel H., Wilson W.E., Cleary M.N., Cooke D.J. & Thomasson P. 1981, å, 100, 209
Hinshaw, G., et al. 2003, ApJS, 148, 135
Hinshaw, G., et al. 2007, ApJS, 170, 288
Jarosik, N., et al. 2003, ApJS, 145, 413
Jewell, J., Levin, S., & Anderson, C. H. 2004, ApJ, 609, 1
Larson, D. L., Eriksen, H. K., Wandelt, B. D., Górski, K. M., Huey, G., Jewell, J. B., & O'Dwyer, I. J. 2007, ApJ, 656, 653
Lewis, A., & Bridle, S. 2002, Phys. Rev. D, 66, 103511
O'Dwyer, I. J. et al. ApJ, 617, L99
Page, L., et al. 2007, ApJS, 170, 335
Spergel, D. N., et al. 2007, ApJS, 170, 377
Wandelt, B. D., Larson, D. L., & Lakshminarayanan, A. 2004, Phys. Rev. D, 70, 083511